Hyperspectral and Multispectral Ocean Versions of ATREM Codes

Bo-Cai Gao

October 2018

Remote Sensing Division, Code 7230
Naval Research Laboratory, Washington, DC USA

Brief History on ATREM Algorithm Development

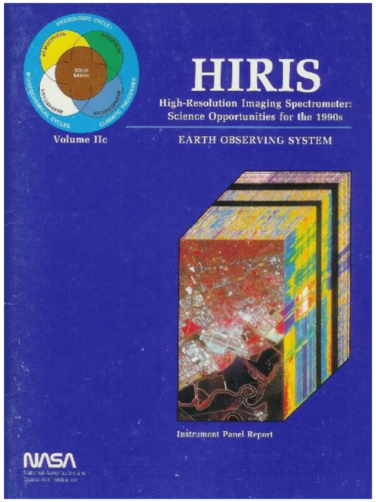

HIRIS
High-Resolution Imaging Spectrometer:
Science Opportunities for the 1990s
Volume IIc
EARTH OBSERVING SYSTEM
Instrument Panel Report
NASA
National Aeronautics and
Space Administration

We started to develop the first land version of hyperspectral atmospheric correction code at U. of Colorado in Boulder in late 1980s to support the ill-fated NASA HIRIS Project. In this version of ATREM code, the 5S code was used to model Rayleigh and aerosol scattering effects, while the Malkmus narrow band model was used to simulate atmospheric gas absorption effects. for calculations. We used a narrow band model to model atmospheric gas absorption bands.
The ATREM source code was publicly released through U. of Colorado to more than 300 researchers worldwide in mid-1990s.

Timeline of algorithm development:

- ATREM – 1st land version (~1991, band model) to support the AVIRIS/HIRIS Project.
- ATREM – upgraded land version (~1997, line-by-line model & 6S) to support the Navy COIS/NEMO Project.
- ATREM – 1st ocean version (~1999, line-by-line, spectrum matching using ***channels above 0.86 μm for Case 2 waters***, based on R. Fraser's formulation and multi-layer atmospheric model).
- ATREM for MODIS – Developed in early 2000s with financial support from SIMBIOS Project, delivered the code to NASA GSFC, but not used by NASA.
- In more recent years, we made major upgrades to the hyperspectral version of ATREM code, e.g., extending lookup tables to cover UV spectral range (350 – 400 nm) & replacing the extra-terrestrial solar irradiance curve. We also developed various versions of multi-channel ATREM codes to process data from VIIRS, Landsat 8 OLI, Sentinel 2 MSI, GOCI, GOES-R ABI, DSCOVR EPIC data, etc. We supported the NASA HyspIRI Airborne Field Campaigns, AVIRIS-NG India Campaigns, NASA CORAL, and NSF ORCAS.

Selected Publications On Atmospheric Corrections

- **1993** - Gao, B.-C., K. H. Heidebrecht, and A. F. H. Goetz, Derivation of scaled surface reflectances from AVIRIS data, *RSE., 44*, 165-178.

- **2000** - Gao, B.-C., et al., Atmospheric correction algorithm for hyperspectral remote sensing of ocean color from space, Appl. Opt., 39, 887-896.
- **2007 -** Gao, B.-C., M. J. Montes, R.-R. Li, H. M. Dierssen, and C. O. Davis, An atmospheric correction algorithm for remote sensing of bright coastal waters using MODIS land and ocean channels in the solar spectral region, TGRS, 45, 1835-1843.

- **2009** - Atmospheric correction algorithms for hyperspectral remote sensing data of land and ocean, RSE, 113, S17-S24.
- **2003** - Li, R.-R., Y. J. Kaufman, B.-C. Gao, and C. O. Davis, Remote sensing of suspended sediments and shallow coastal waters, TGRS, 41, 559-566, 2003.

- 2017 – Gao, B.-C., and R.-R. Li, Removal of thin cirrus scattering effects in Landsat 8 OLI images using the cirrus detecting channels, Remote Sensing, 9, 834, 2017.

Adopting R. Fraser Formulation

$$\begin{aligned}
L_t = {} & L_0(\lambda; \theta, \phi; \theta_0, \phi_0; z_{sen}, z_{sfc} ; \tau_a) + \\
& L_{\mathrm{sfc}}(\lambda; \theta, \phi; \theta_0, \phi_0; z_{sen}, z_{sfc} ; \tau_a; W)\, t(\lambda; \theta; z_{sen}, z_{sfc} ; \tau_a) + \\
& L_{\mathrm{w}}(\lambda; \theta, \phi; \theta_0, \phi_0; W; C)\, t'(\lambda; \theta; z_{sen}, z_{sfc} ; \tau_a)
\end{aligned}$$

L_t = measured radiance

L_0 = path radiance (i.e., atmospheric scattering)

L_{sfc} = direct and diffuse radiance reflected off ocean surface

L_{w} = water (or ground) leaving radiance

t = diffuse + direct upward transmission

t' = diffuse upward transmission

τ_a = aerosol optical properties

W = wind speed

C = water column and bottom constituents

θ, ϕ = view zenith and azimuth angles

θ_0, ϕ_0 = solar zenith and azimuth angles

z_{sen} , z_{sfc} = sensor and surface altitudes

Relevant Equations and Definitions

In the absence of gas absorption, the radiance at the satellite level is:

$$L_{obs} = L_0 + L_{sfc}\, t'_u + L_w\, t_u, \tag{1}$$

L_0: path radiance; L_w: water leaving radiance;

L_{sfc}: radiance reflected at water surface; t_u: *upward transmittance*

Define $$L_{atm+sfc} = L_0 + L_{sfc}\, t'_u \tag{2}$$

Eq. (1) becomes: $$L_{obs} = L_{atm+sfc} + L_w\, t_u \tag{3}$$

Multiply Eq. (3) by π and divide by $(\mu_0\, E_0)$, Eq. (3) becomes:

$$\pi\, L_{obs} / (\mu_0\, E_0) = \pi\, L_{atm+sfc} / (\mu_0\, E_0) + \pi\, L_w\, t_d\, t_u / (\mu_0\, E_0\, t_d) \tag{4}$$

Several reflectances are defined as:

Satellite apparent reflectance: $$\rho^*_{obs} = \pi\, L_{obs} / (\mu_0\, E_0), \tag{5}$$

$$\rho^*_{atm+sfc} = \pi\, L_{atm+sfc} / (\mu_0\, E_0), \tag{6}$$

Water leaving reflectance: $$\boldsymbol{\rho_w = \pi\, L_w / (\mu_0\, E_0\, t_d) = \pi\, L_w / E_d} \tag{7}$$

Remote sensing reflectance: $$\mathbf{R_{rs}} = \boldsymbol{\rho_w / \pi = L_w / E_d} \tag{7'}$$

Substitute Eqs (5) – (7) into Eq. (4): $$\rho^*_{obs} = \rho^*_{atm+sfc} + \rho_w\, t_d\, t_u \tag{8}$$

After consideration of gas absorption and multiple reflection between the atmosphere and surface and with further manipulation, we can get:

$$\rho_w = (\rho^*_{obs}/T_g - \rho^*_{atm+sfc}) / [t_d\, t_u + s\, (\rho^*_{obs}/T_g - \rho^*_{atm+sfc})] \tag{11}$$

Gao, B.-C., M. J. Montes, Z. Ahmad, and C. O. Davis, Atmospheric correction algorithm for hyperspectral remote sensing of ocean color from space, Appl. Opt., 39, 887-896, February 2000.

Simulation of Sunglint Effects

Using Ahmad and Fraser RT code to generate lookup tables

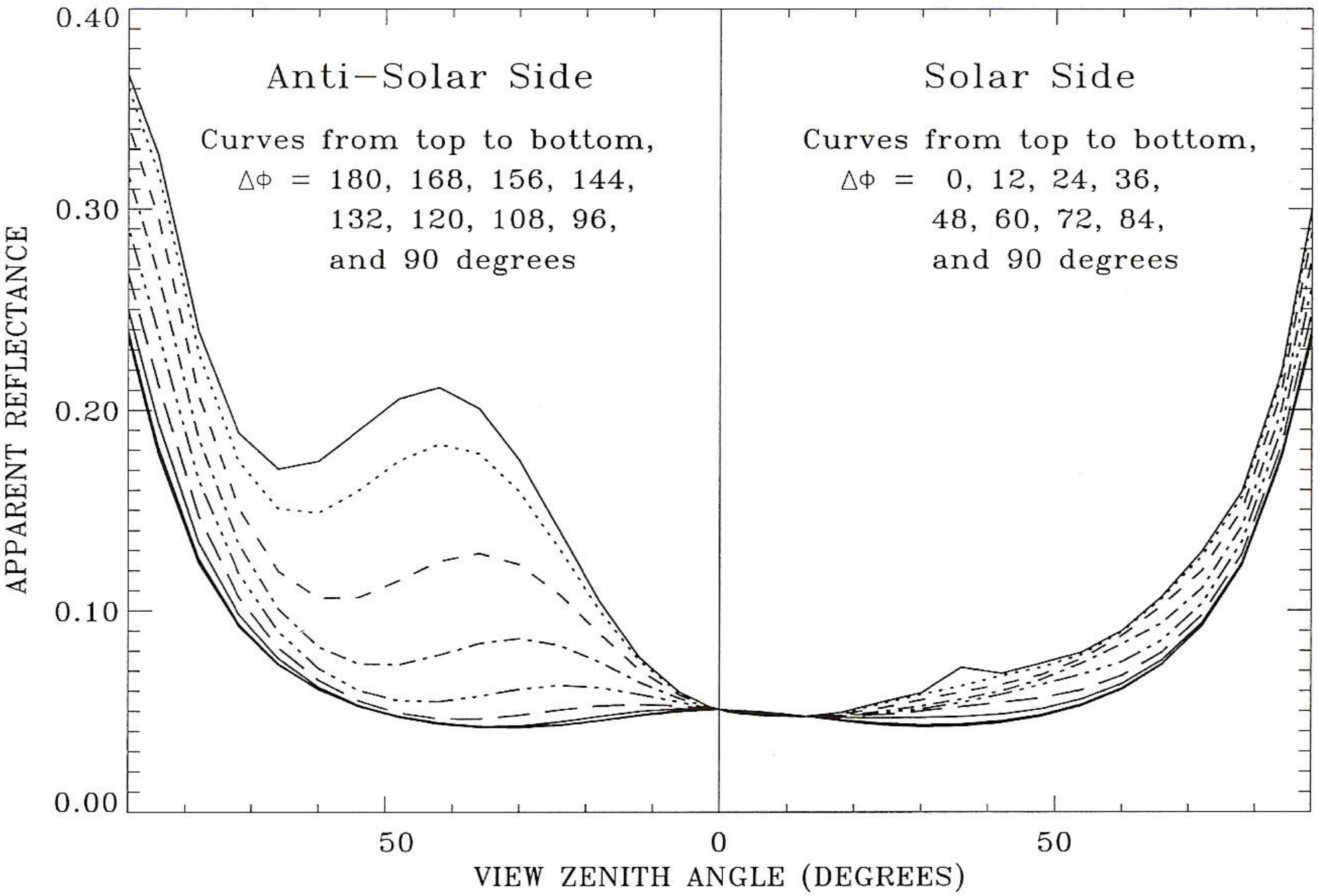

Wavelength: 0.61 micron

Coastal Waters Are Dark Above 0.86 Micron (AVIRIS Norfork Images)

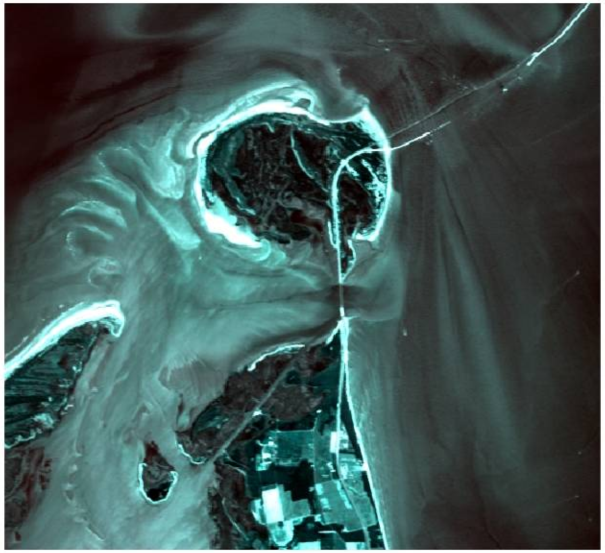
RGB (0.66, 0.55, 0.47 μm)

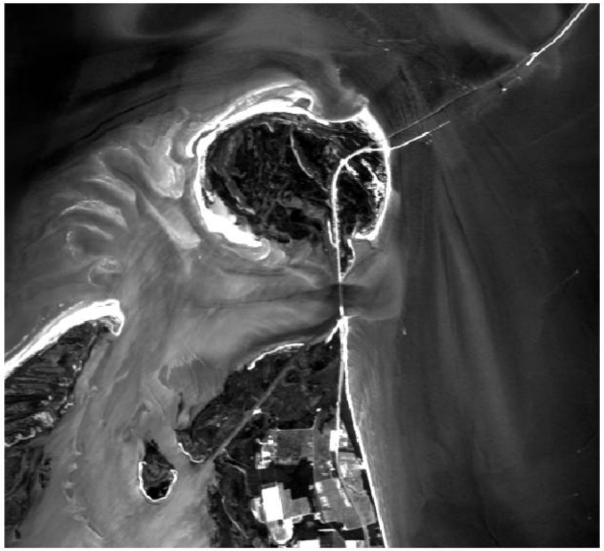
0.55-μm

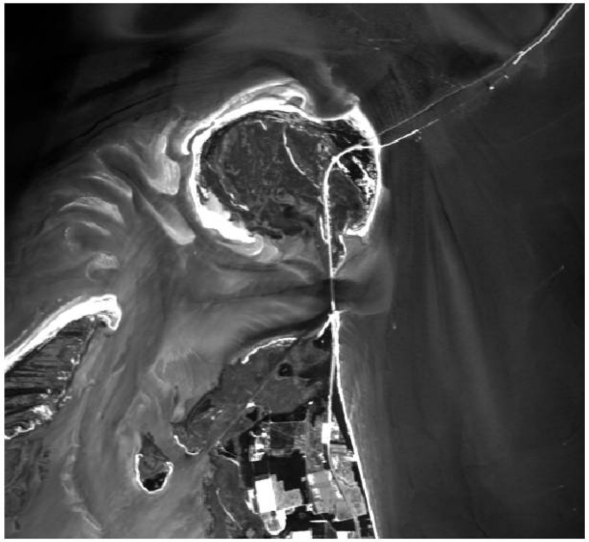
0.66-μm

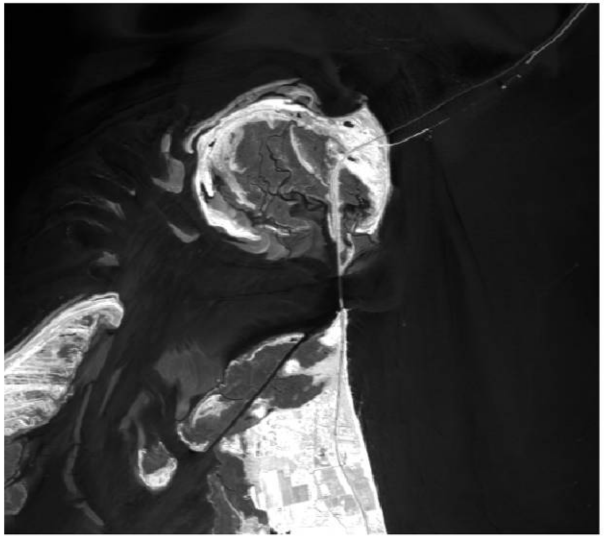
0.75-μm

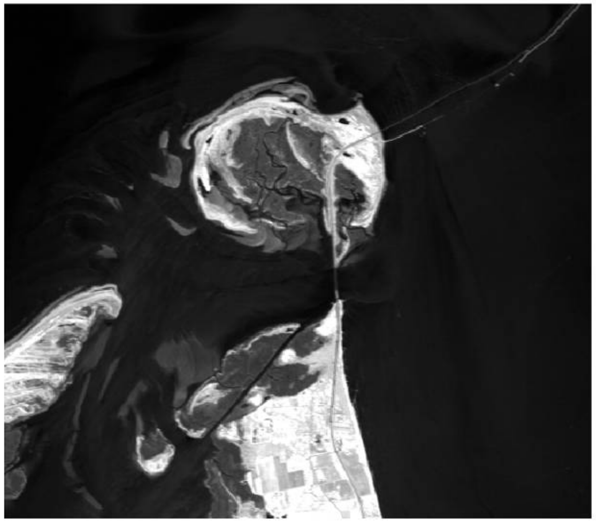
0.86-μm

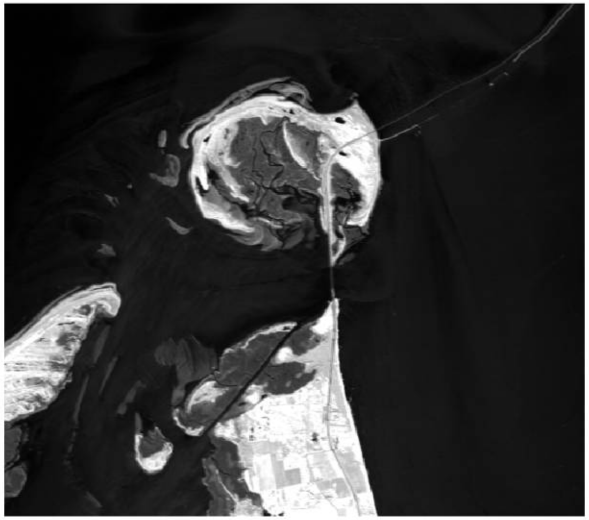
1.02-μm

Atmospheric Correction for Water Surfaces

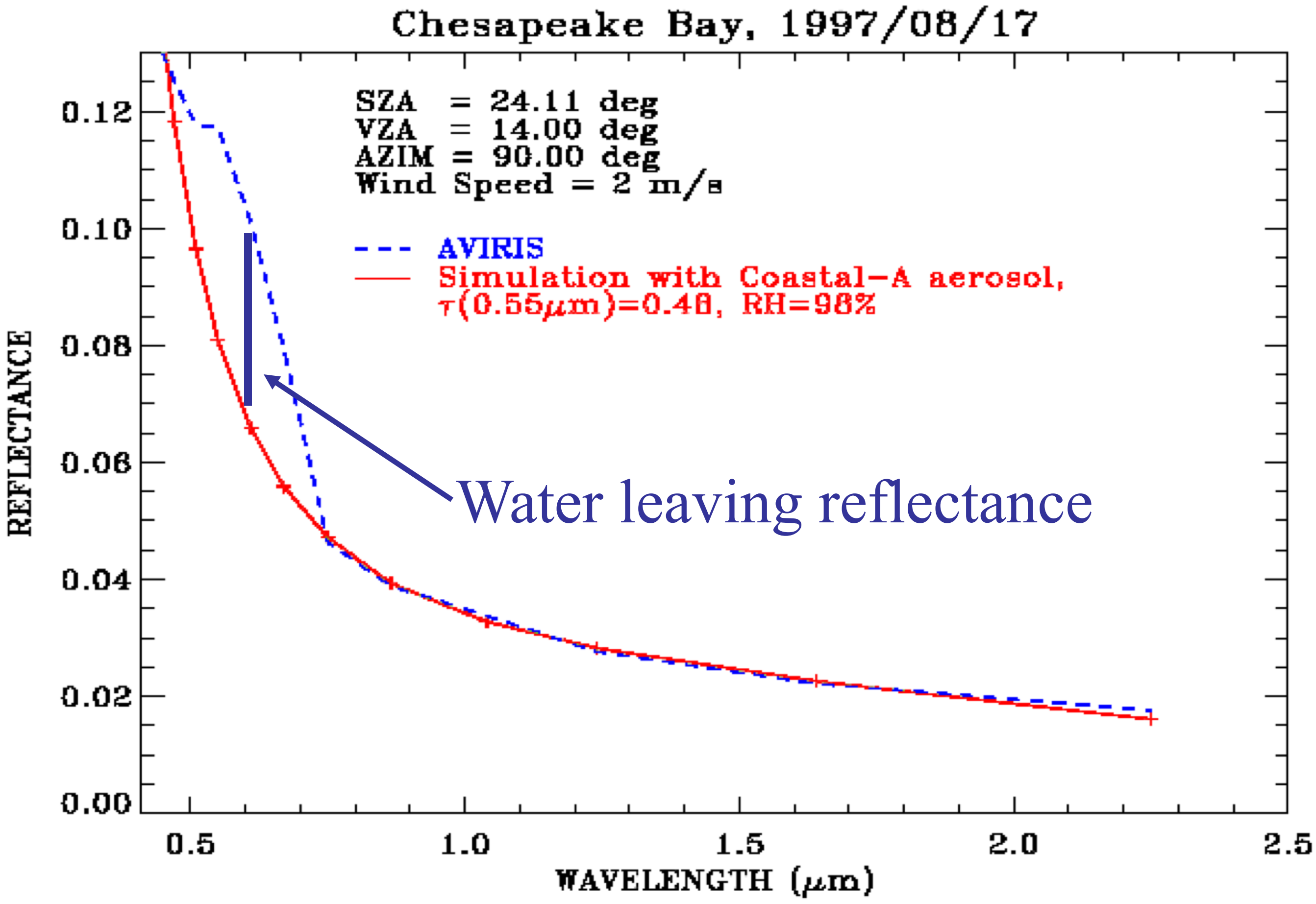

Water leaving reflectance

Channels at 0.86 and longer wavelengths are used to estimate atmospheric effects, and then extrapolate to the visible region. The differences between the two curves above are proportional to water leaving reflectances.

Sample Retrieval Results From PRISM Data & Comparison with Ground Measurements

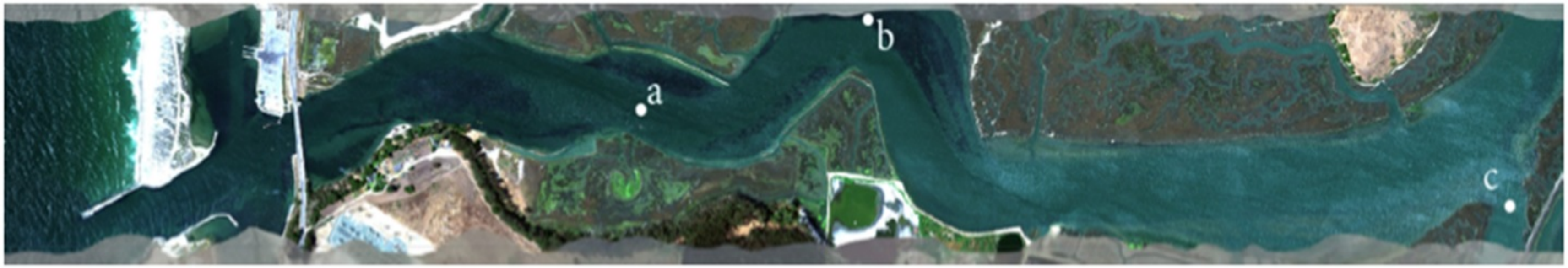

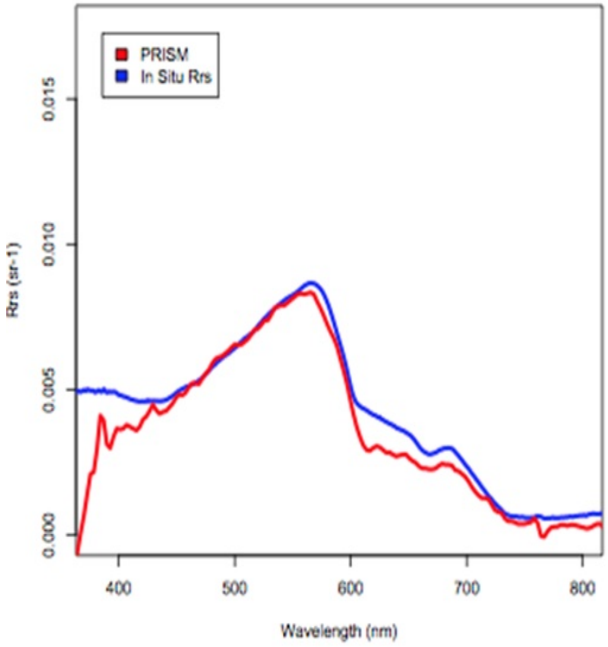

(a) West LOBO Buoy

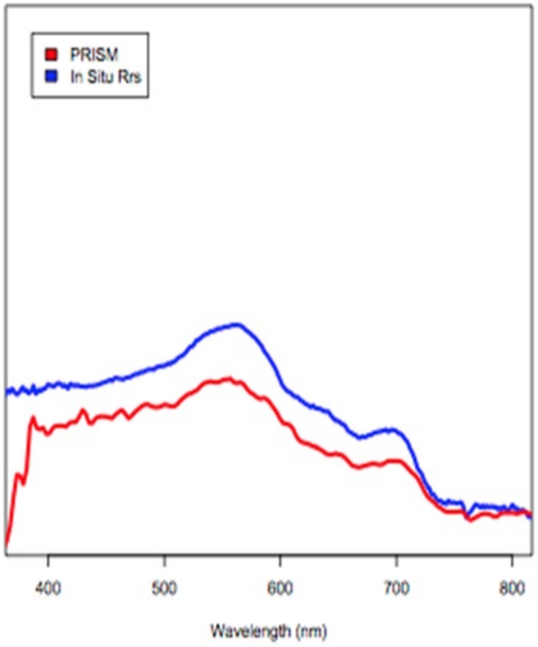

(b) Seal Bend Dense Eelgrass

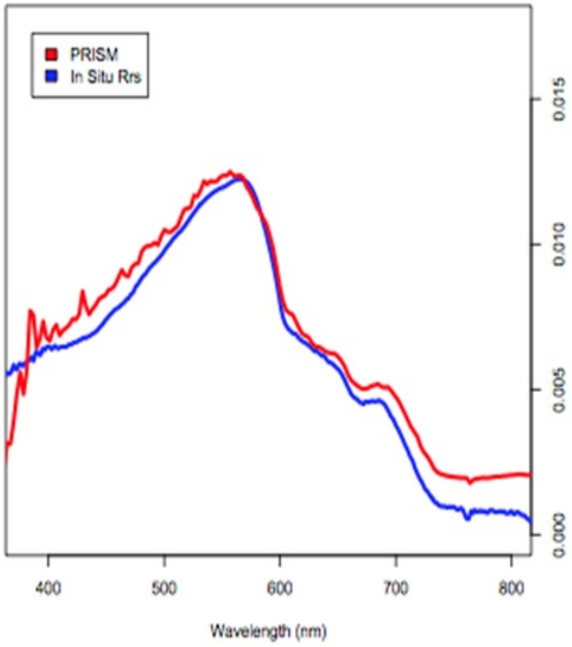

(c) East LOBO Buoy

Sample VIIRS Ocean Color Results

(A)

(B)

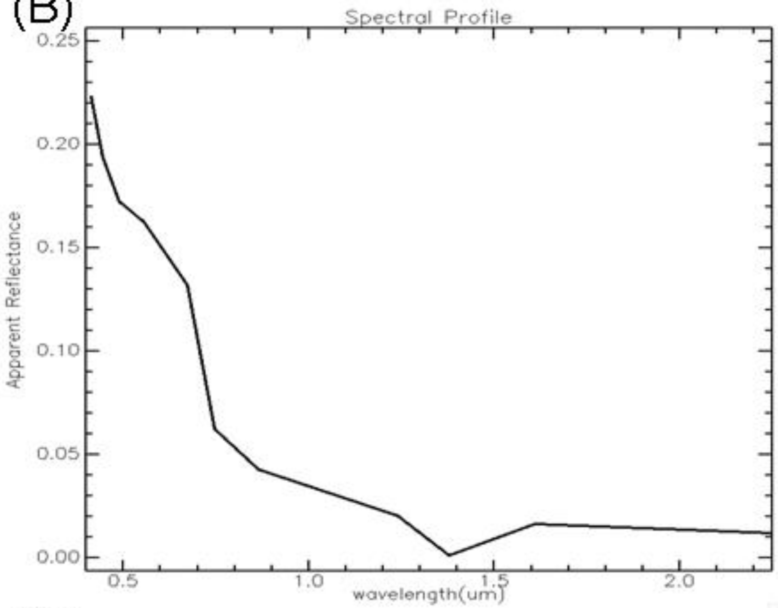

(C)

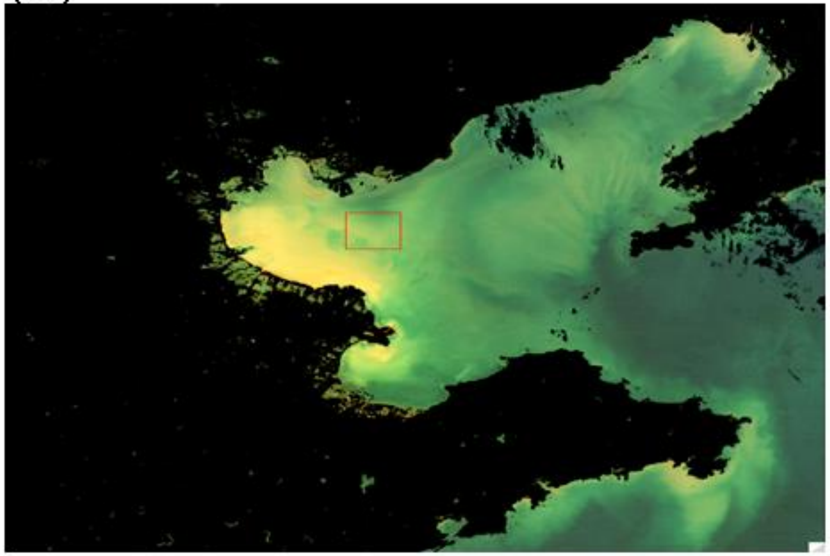

(D)

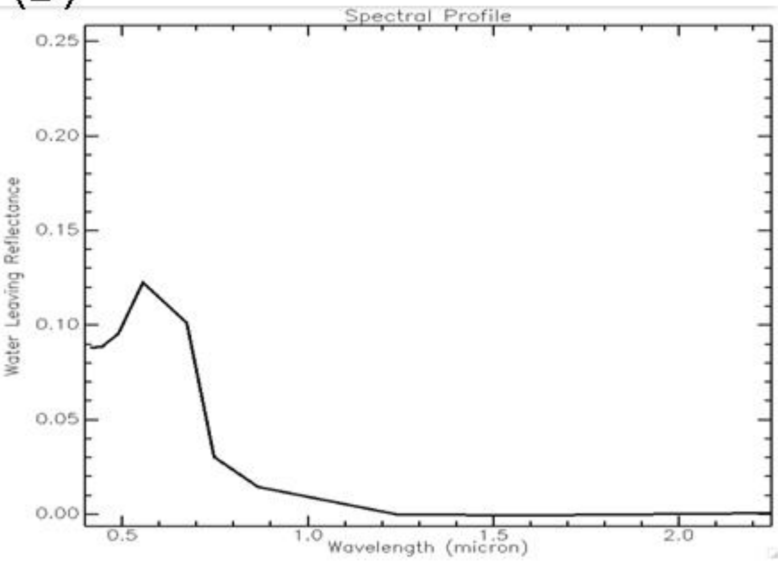

Sample Landsat 8 OLI Ocean Color Results

RGB Image

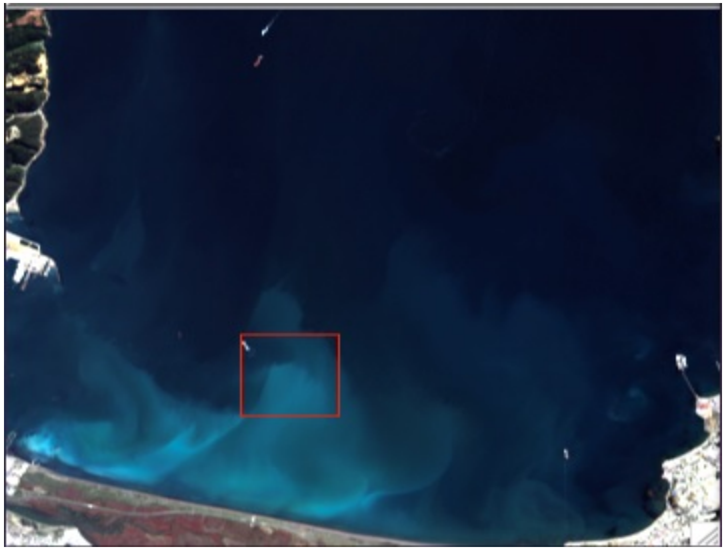

Corrected RGB Image

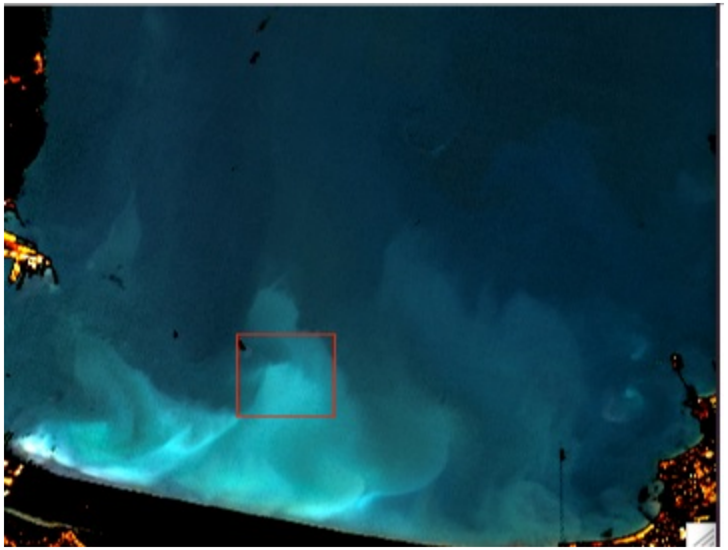

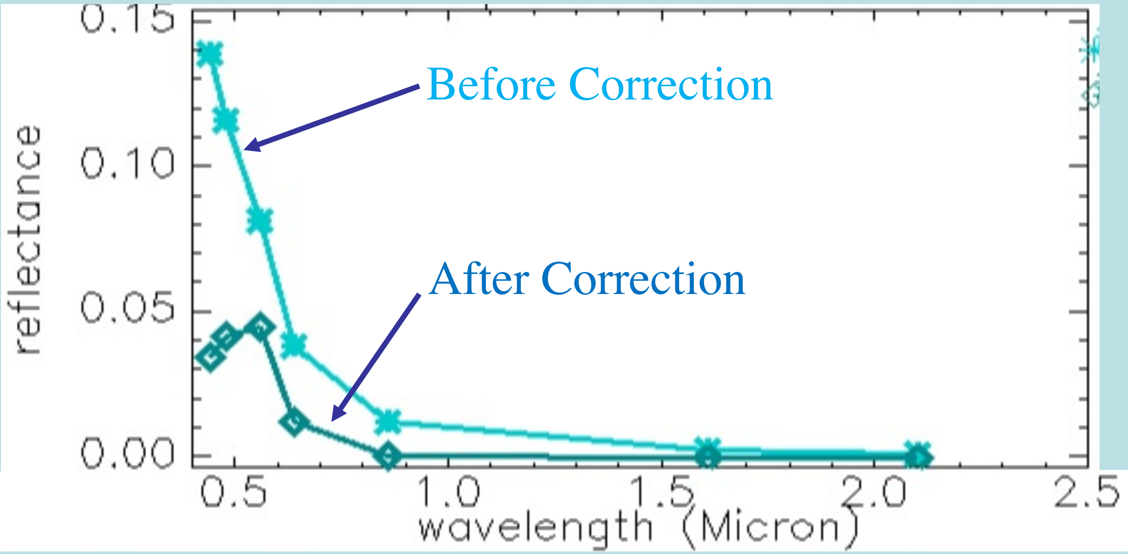

Before Correction

After Correction

Sample Landsat 8 OLI Cirrus Correction

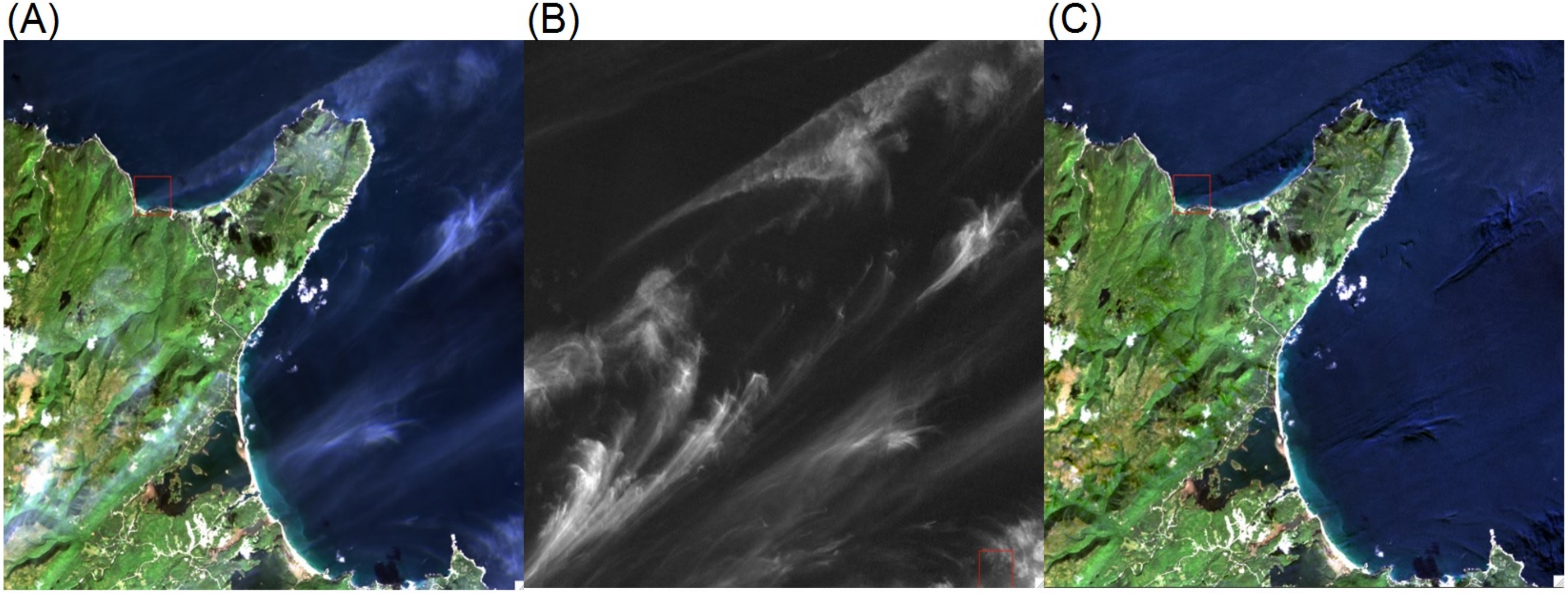

Cirrus correction should, in principle, be made prior to the normal atmospheric corrections.